Inorganic Chemistry

Article

pubs.acs.org/IC

Thermodynamically Metastable Thiocyanato Coordination Polymer That Shows Slow Relaxations of the Magnetization

Julia Werner,[†] Michał Rams,[‡] Zbigniew Tomkowicz,[‡] Tomče Runčevski,[§] Robert E. Dinnebier,[§] Stefan Suckert,[†] and Christian Näther*[,†]

[†]Institut für Anorganische Chemie, Christian-Albrechts-Universität zu Kiel, Max-Eyth-Straße 2, 24118 Kiel, Germany

[‡]Institute of Physics, Jagiellonian University, Łojasiewicza 11, 30-348 Kraków, Poland

[§]Max Planck Institute for Solid State Research, Heisenbergstraße 1, 70569 Stuttgart, Germany

Supporting Information

ABSTRACT: Reaction of cobalt thiocyanate with 4-acetylpyridine leads to the formation of $[Co(NCS)_2(4\text{-acetylpyridine})_2]_n$ (**3/I**). In its crystal structure the Co cations are connected by pairs of μ-1,3-bridging thiocyanato ligands into dimers that are further connected into layers by single anionic ligands. DTA-TG measurements of $Co(NCS)_2(4\text{-acetylpyridine})_4$ (**1**) led to the formation of **3/I**. In contrast, when the hydrate $Co(NCS)_2(4\text{-acetyl-pyridine})_2(H_2O)_2$ (**2**) is decomposed, a mixture of **3/I** and a thermodynamically metastable form **3/II** is obtained. Further investigations reveal that thermal annealing of **2** leads to the formation of **3/II**, that contains only traces of the stable form **3/I**. DSC and temperature dependent X-ray powder diffraction (XRPD) measurements prove that **3/II** transforms into **3/I** on heating. The crystal structure of **3/II** was determined ab initio from XRPD data. In its crystal structure the Co cations are linked by pairs of bridging thiocyanato anions into a 1D coordination polymer, and thus, **3/II** is an isomer of **3/I**. Magnetic measurements disclose that the stable form **3/I** only shows paramagnetism without any magnetic anomaly down to 2 K. In contrast, the metastable form **3/II** shows ferromagnetic behavior. The phase transition into ordered state at T_c = 3.8 K was confirmed by specific heat measurements. Alternating current susceptibility measurements show frequency dependent maxima in χ' and χ'', which is indicative for a slow relaxation of the magnetization.

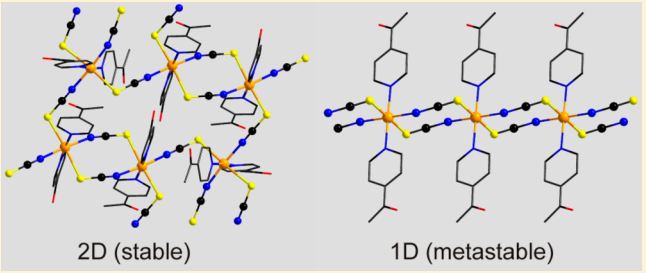

INTRODUCTION

Investigations on a rational synthesis of new compounds with desired, e.g., magnetic properties are an important field in chemical research.

This approach, often called "crystal engineering", is based on investigations on the structure−property relationships of crystalline solids and on considerations for how a specific structure can be prepared.[1] In this context one has to be aware of the phenomena of polymorphism or isomerism that are frequently observed, which makes the prediction of a coordination network challenging.[2]

Recently, we have reported on the synthesis of new coordination polymers based on transition metal thiocyanates and neutral N-donor coligands. In the course of these investigations we prepared a number of compounds in which the metal cations are octahedrally coordinated by four μ-1,3-bridging anionic ligands and two N-donor coligands. In those cases where monodentate coligands are used, 1D coordination polymers are frequently obtained, whereas using bidentate coligands mostly leads to the formation of 2D structures.[3] In all of these compounds the metal cations are connected by μ-1,3-bridging anionic ligands into chains (Figure 1), which obviously corresponds to a relatively stable arrangement, usually observed in such compounds.[4] In a few cases, 2D thiocyanato coordination networks are obtained, in which two metal cations are μ-1,3-bridged into dimers by pairs of thiocyanato anions which are then further connected into layers by μ-1,3-bridging single anionic ligands.[5]

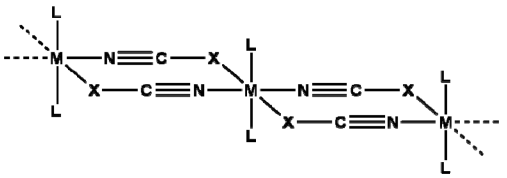

Figure 1. View of the metal thiocyanato chains usually observed in compounds of composition $M(NCX)_2(L)_2$ with M = Mn, Fe, Co, and Ni, X = S, Se and L = monodentate N-donor coligand.

Magnetic investigations on the 1D compounds $[M(NCS)_2(pyridine)_2]_n$ with $M = Mn^{II}$, Fe^{II}, Co^{II}, and Ni^{II} reveal that the Mn compound shows antiferromagnetic ordering, whereas for the Ni and for the Fe compounds reported in the literature, a metamagnetic transition is observed.[6] Instead, $[Co(NCS)_2$-

Received: December 18, 2014
Published: March 5, 2015

DOI: 10.1021/ic503029t
Inorg. Chem. 2015, 54, 2893−2901

$(pyridine)_2]_n$ shows a slow relaxation of the magnetization indicating a single chain magnetic (SCM) behavior.[7] This is a relatively rare magnetic behavior with potential for future applications, and this is one of the reasons why an increasing number of such compounds were recently reported in the literature.[8]

In further work we have prepared a large number of such μ-1,3-bridging thiocyanato coordination polymers and investigated the influence of the metal cation, the anionic ligand, and the coligand on their structural and magnetic properties. Surprisingly, in $[Co(NCS)_2(pyridine)_2]_n$, the anionic ligand can be exchanged by selenocyanato anions and the coligand by, e.g., 4-ethylpyridine without losing the magnetic relaxations.[9] A similar magnetic behavior was also observed in $[Fe(NCSe)_2(pyridine)_2]_n$ that compared to the thiocyanato analog exhibits stronger intrachain interactions.[10] Because of the actual interest in such magnetic behavior our research mainly focused on compounds that contain cations of large magnetic anisotropy like, e.g., Fe^{II} and Co^{II}. In this context it is noted that the compounds with a 2D thiocyanato network do not show slow relaxations and, therefore, are of minor importance.[5]

To study the influence of the substitution of the pyridine coligands on the magnetic properties we tried to prepare compounds based on cobalt(II) thiocyanate with 4-acetylpyridine as a ligand. Two discrete complexes of composition $Co(NCS)_2(4\text{-acetylpyridine})_4$ (**1**) and $Co(NCS)_2(4\text{-acetylpyridine})_2(H_2O)_2$ (**2**) are already reported in literature; however, the desired compound $[Co(NCS)_2(4\text{-acetylpyridine})_2]_n$ was unknown.[11] We have found that a compound of this chemical composition can easily be prepared in solution, but instead of the 1D structure, a 2D thiocyanato network was obtained, which showed only paramagnetic behavior. In a consecutive work, we were able to prepare the desired 1D compound that showed relaxations of the magnetization, and we have found that it is metastable at room temperature with the 2D polymorph being the thermodynamically stable form. Herein we report on these investigations.

EXPERIMENTAL SECTION

Synthesis. 4-Acetylpyridine and $Co(NCS)_2$ were obtained from Alfa Aesar. Solvents were used without further purification. Crystalline powders of compounds **1**, **2**, and **3/I** were prepared by stirring the reactants in appropriate solvents at room temperature. Compound **3/II** was prepared by annealing at 70 °C. The purity of all compounds was proved by XRPD and elemental analysis.

Synthesis of Compound 1. $Co(NCS)_2$ (43.8 mg, 0.25 mmol), and 4-acetylpyridine (275.3 μL, 2.50 mmol) were stirred in 2.0 mL of water for 3 d. Yield: 60.8%. Anal. Calcd (%) for $C_{30}H_{28}CoN_6O_4S_2$: C 54.62, H 4.28, N 12.74; S 9.72. Found: C 54.39, H 4.13, N 12.68, S 9.61. IR (ATR): ν_{max} = 3043 (w), 2905 (w), 2060 (s), 1693 (s), 1555 (m), 1412 (m), 1361 (m), 1262 (s), 1011 (m), 828 (s), 591 (s), 483 (m).

Synthesis of Compound 2. $Co(NCS)_2$ (43.8 mg 0.25 mmol), and 4-acetylpyridine (55.1 μL, 0.50 mmol) were stirred in 1.5 mL of water for 3 d. Yield: 92.6%. Anal. Calcd (%) for $C_{16}H_{18}CoN_4O_4S_2$: C 42.38, H 4.00, N 12.36; S 14.14. Found: C 42.50, H 3.95, N 12.42, S 14.50. IR (ATR): ν_{max} = 3314 (b), 3228 (b), 3046 (w), 2088 (s), 1680 (s), 1557 (m), 1412 (m), 1362 (m), 1276 (s), 1060 (m), 1012 (m), 831 (s), 595 (s), 471 (s).

Synthesis of Compound 3/I. $Co(NCS)_2$ (43.8 mg, 0.25 mmol), and 4-acetylpyridine (55.1 μL, 0.50 mmol) were stirred in 1.5 mL of ethanol for 3 d. Yield: 80.4%. Single crystals suitable for single crystal X-ray diffraction were prepared by the same method in acetonitrile. After 2 weeks dark red single crystals were obtained. Anal. Calcd (%) for $C_{16}H_{14}CoN_4O_2S_2$: C 46.04, H 3.38, N 13.42; S 15.37. Found: C 46.07, H 3.32, N 13.47, S 15.39. IR (ATR): ν_{max} = 3131 (w), 3083 (w), 3046 (w), 2102 (s), 1687 (s), 1555 (m), 1413 (s), 1361 (m), 1270 (s), 1138 (b), 1059 (m), 815 (s), 594 (s), 465 (m).

Synthesis of Compound 3/II. A 60 mg portion of compound **2** was annealed at 70 °C for 1 day. Anal. Calcd (%) for $C_{16}H_{14}CoN_4O_2S_2$: C 46.04, H 3.38, N 13.42; S 15.37. Found: C 46.35, H 3.30, N 13.44, S 14.93. IR (ATR): ν_{max} = 3116 (w), 3078 (w), 2359 (w), 2098 (s), 1697 (s), 1555 (m), 1411 (m), 1360 (m), 1263 (s), 1060 (m), 1014 (m), 818 (s), 593 (s), 469 (m).

Elemental Analysis. CHNS analysis was performed using an EURO EA elemental analyzer, fabricated by EURO VECTOR Instruments and Software.

IR Spectroscopy. FT IR spectra were recorded on a Genesis series FTIR spectrometer, by ATI Mattson, in KBr pellets, as well with an Alpha IR spectrometer from Bruker equipped with a Platinum ATR QuickSnap sampling module between 4000 and 375 cm^{-1}.

Single Crystal X-ray Diffraction. Data collection for **3/I** was performed with an imaging plate diffraction system IPDS-2 with Mo Kα radiation from STOE & CIE. The structure solution was performed with direct methods using SHELXS-97, and structure refinements were performed against F^2 using SHELXL-97. All non-hydrogen atoms were refined with anisotropic displacement parameters. The hydrogen atoms were positioned with idealized geometry and were refined with fixed isotropic displacement parameters [$U_{iso}(H) = -1.2 \cdot U_{eq}(C_{aromatic})$ using a riding model. Selected crystal data are shown in Table 1. CCDC 1030910 (**3/I**) and CCDC 1030911 (**3/II**) contain the supplementary crystallographic data for this Article. These data can be obtained free charge from the Cambridge Crystallographic Data Centre via http://www.ccdc.cam.ac.uk/data_request/cif.

Table 1. Selected Crystal Data and Details of the Structure Refinement for Compound 3/I

	3/I
formula	$C_{16}H_{14}CoN_4O_2S_2$
MW/g mol^{-1}	417.36
cryst syst	*orthorhombic*
space group	*Pbca*
a/Å	9.5315(3)
b/Å	15.8242(4)
c/Å	24.3712(6)
α/deg	90
β/deg	90
γ/deg	90
V/Å^3	3675.87(17)
T/K	293(2)
Z	8
D_{calc}/g cm^{-3}	1.508
μ/mm^{-1}	1.177
θ_{max}/deg	2.57−28.07
measured reflns	32 860
unique reflns	4408
reflns [$F_0 > 4\sigma(F_0)$]	3747
parameter	228
R_{int}	0.0462
R1 [$F_0 > 4\sigma(F_0)$]	0.0539
wR2 [all data]	0.0962
GOF	1.262
$\Delta\rho_{max}$, $\Delta\rho_{min}$/e Å^{-3}	0.281/−0.302

X-ray Powder Diffraction. For checking samples' phase purity, XRPD experiments were performed using a Stoe Transmission Powder Diffraction System (STADI P) with Cu Kα radiation (λ = 154.0598 pm) that is equipped with a linear position-sensitive detector (6.5−7° simultaneous; scan range overall = 2−130°) from STOE & CIE, an Image Plate Detector (scan range overall = 0−127°), and a

DOI: 10.1021/ic503029t
Inorg. Chem. 2015, 54, 2893−2901

PANalytical X'Pert Pro MPD Reflection Powder Diffraction System with Cu Kα radiation (λ = 154.0598 pm) equipped with a PIXcel semiconductor detector from PANalytical.

For the crystal structure solution of **3/II** and for the in situ measurements a D8 Advance powder diffractometer was used [Bruker, Cu Kα1, radiation from primary Ge(111)-Johannson-type monochromator, Vantag-1 position sensitive detector (PSD), with an opening angle of 6° in Debye−Scherrer geometry]. The powdered sample was sealed in a borosilicate glass capillary (0.5 mm diameter Hilgenberg glass capillary No. 50), which was spun during the measurement for better data statistics. For the crystal structure, solution data were taken from 6° to 43° 2θ for a period of 24 h. For the temperature-variable measurements data were collected at 5 K temperature intervals, from 8° to 28° 2θ for a period of 15 min.

The powder pattern of **3/II** was analyzed with TOPAS 4.2.[12] The indexing was performed from first-principles by the iterative use of singular value decomposition. The indexing indicated the phase crystallizes in a triclinic unit cell. Precise lattice parameters were determined by a Pawley fit.[13] The crystal structure determination was performed in the $P1$ and $P\bar{1}$ space groups with the simulated annealing approach where the cation was positioned at 1/2 1/2 1/2 special position and the organic ligands were allowed to freely rotate and translate.[14] For the final Rietveld refinement,[15] all profile and lattice parameters were subjected to free unconstrained refinement, and the final plot is shown in Figure S1 in the Supporting Information. Selected crystallographic data are listed in Table 2. The positions of the hydrogen atoms were calculated.

Table 2. Selected Crystal Data and Details of the Rietveld Refinement for Compound 3/II

	3/II
formula	$C_{16}H_{14}CoN_4O_2S_2$
cryst syst	triclinic
space group	$P\bar{1}$
a/Å	5.628 03(64)
b/Å	8.4717(14)
c/Å	10.3170(19)
α/deg	76.7846(97)
β/deg	87.540(15)
γ/deg	73.483(17)
V/Å^3	458.988
T/K	297.15
Z	1
start to finish angle/deg 2θ	6−43
λ/Å	1.540 596
R_{wp}/%[a]	7.40
R_p/%[a]	11.54
R_{exp}/%[a]	10.27
R_{Brag}/%[a]	0.25

[a]Background corrected values. The lower R_{wp} value compared to R_p is attributed to an inappropriate weighting scheme for data collected with Mythen PSD.

Differential Thermoanalysis and Thermogravimetry. The DTA-TG measurements were performed in a nitrogen atmosphere (purity: 5.0) in Al_2O_3 crucibles using a STA-409CD instrument from Netzsch. The DTA-TG-MS measurements were performed with the same instrument, which is connected to a quadrupole mass spectrometer from Balzers via Skimmer coupling from Netzsch. The MS measurements were performed in analog and trend scan mode in Al_2O_3 crucibles in a dynamic nitrogen atmosphere (purity: 5.0) using heating rates of 4 K/min. All measurements were performed with a flow rate of 75 mL/min. The instrument was calibrated using standard reference materials.

Magnetic Measurements. Magnetic measurements of **1**, **2**, and **3/I** were performed using Quantum Design PPMS equipped in 7 T magnet, using samples mounted in a gelatin capsule.

For **3/II** the magnetic measurements were performed using a Quantum Design MPMS-5XL magnetometer. The powder sample was pressed into 5 mm × 0.8 mm pellet together with a bag made of PTFE tape. The pellet was oriented along the magnetic field to minimize the demagnetization effect. The diamagnetic response of the PTFE and the core diamagnetic response were subtracted.

Specific Heat. Specific heat measurements were performed using the relaxation technique in Quantum Design PPMS cryostat. The powder sample was pressed into 2.4(1) mg, 3 mm diameter pellet with no binder. The heat capacity of the microcalorimeter, together with a drop of ApiezonN grease used to fix the sample, was measured before the sample measurement and subtracted. The influence of the magnetic field on this background signal is negligible above 2 K.

RESULTS AND DISCUSSIONS

Synthetic Aspects. In the beginning of our investigations, cobalt(II) thiocyanate was reacted in various solvents with different stoichiometric ratios of 4-acetylpyridine, and the products obtained were characterized by elemental analysis, IR spectroscopy, and X-ray powder diffraction (XRPD). We have found that in water only a 6-fold excess of the coligand leads to the formation of $Co(NCS)_2$(4-acetylpyridine)$_4$ (**1**) whereas all other stoichiometric ratios led to the formation of the hydrate $Co(NCS)_2$(4-acetylpyridine)$_2(H_2O)_2$ (**2**) (Table S1 in the Supporting Information). IR spectroscopic investigations show that the asymmetric $\nu_{(as)}$ C−N stretching vibration is observed at 2060 cm^{-1} for **1** and at 2088 cm^{-1} for **2** indicating that the anionic ligands are only terminal N-bonded (Figures S2 and S3 in the Supporting Information).[16] In contrast, in ethanol, methanol, and acetonitrile in most cases a new crystalline compound (**3/I**) crystallized. The results of elemental analysis showed that a compound of composition $Co(NCS)_2$(4-acetylpyridine)$_2$ was formed, and in the IR spectra its asymmetric $\nu_{(as)}$ C−N stretching vibration was observed at 2102 cm^{-1}, indicating that μ-1,3 bridging thiocyanato anions are present (Figure S4 in the Supporting Information).[16] Investigations with XRPD revealed that compounds **1** and **2** were obtained as pure crystalline phases and that in the powder pattern of compound **3** no reflections of **1** or **2** are present, indicating that this compound is also obtained as phase pure (Figures S5−S7 in the Supporting Information). Later on, single crystals of compound **3/I** were prepared by reaction of $Co(NCS)_2$ with 4-acetylpyridine in a ratio of 1:2 in acetonitrile, and single crystal X-ray structure analysis confirmed the composition of this compound as $Co(NCS)_2$(4-acetylpyridine)$_2$ (see Experimental Section).

Crystal Structure of Form 3/I. Compound **3/I** crystallizes in the orthorhombic space group *Pbca* with 8 formula units in the unit cell. The asymmetric unit consists of one Co cation, two crystallographically independent thiocyanato anions, and two distinct 4-acetylpyridine ligands (Figure S8 in the Supporting Information). In the crystal structure, the Co cations are always *trans* coordinated by two coligands as well as two N- and two S-bonding thiocyanato anions. The Co−N bond lengths between 2.064(2) and 2.174(2) Å and the Co−S bond lengths of 2.572(1) and 2.647(1) Å are in the typical range for similar compounds, and the bonding angles show a slight distortion from the octahedral geometry (Table S2 in the Supporting Information). Each of the two Co cations is linked by pairs of μ-1,3-bridging thiocyanato anions into dimers, that are further connected by single μ-1,3-bridging anionic ligands

DOI: 10.1021/ic503029t
Inorg. Chem. 2015, 54, 2893−2901

into layers parallel to the *a*-/*b*-plane (Figure 2, top). The layers are stacked perpendicular to the *c*-axis with the acetyl group of

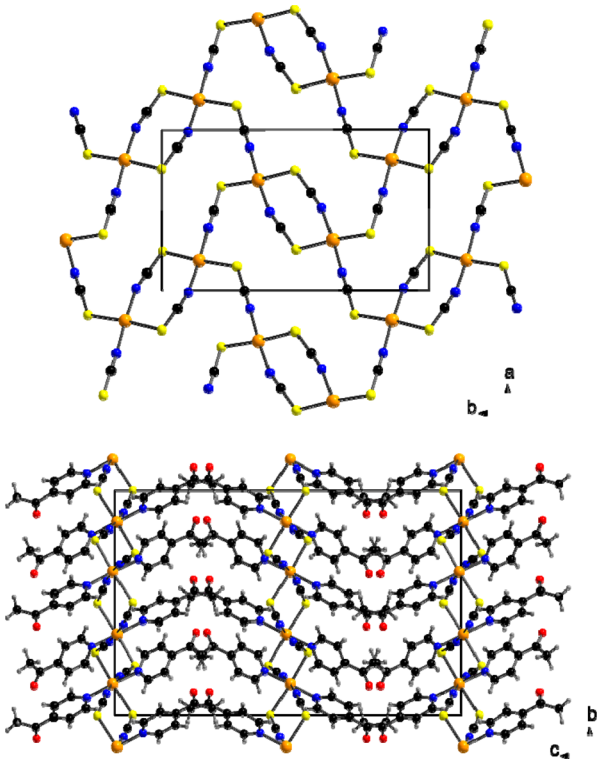

Figure 2. Crystal structure of the compound **3/I** with view of the cobalt thiocyanato network along the *c*-axis (top) and perpendicular to the layers with view along the *a*-axis (bottom). An ORTEP plot of this compound is given in Figure S8 in the Supporting Information.

the coligands pointing to each other. It is noted that the phenyl rings of neighboring chains are shifted relative to each other, which means that no $\pi\cdots\pi$ interactions are observed.

On the basis of the structural data, the powder pattern was calculated, which shows that compound **3/I** was obtained as a pure crystalline phase (Figure S9 in Supporting Information). Surprisingly, this structure is completely different from that expected as no cobalt thiocyanato chains are observed, which is the most common structural motif for such coordination polymers. Considering the 2D structure, it is highly unlikely that this compound will show a slow relaxation of the magnetization of single chains. Since **3/I** is formed by crystallization from solution, it can be assumed that it is the thermodynamic stable product at room temperature. Consequently, the 1D compound (if it exists) must be metastable and therefore not observed by recrystallizations. This modification might be formed by thermal decomposition of suitable precursor compounds like, e.g., the discrete complexes **1** and **2**. Therefore, both compounds were investigated by simultaneous differential thermoanalysis and thermogravimetry (DTA-TG) and temperature dependent XRPD.

Thermoanalytical Measurements of Compounds 1 and 2. If $Co(NCS)_2(4\text{-acetylpyridine})_4$ (**1**) is heated in a thermobalance, a mass step is observed at about 118 °C, which is accompanied by an endothermic event in the DTA curve (Figure 3 and Figure S10 in the Supporting Information). The experimental mass loss of this step of 36.0% is in good agreement with that calculated for the removal of two of the four 4-acetylpyridine ligands. On further heating, a second step

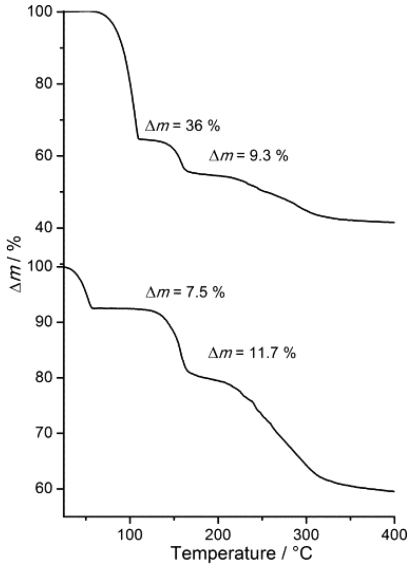

Figure 3. Thermogravimetric curve for compound **1** (top) and **2** (bottom) at 1 K/min.

of 9.3% is observed that cannot be assigned to any reasonable reaction. This result suggests that in the first TG step a compound of composition $Co(NCS)_2(4\text{-acetylpyridine})_2$ has formed. To investigate the nature of this intermediate in more detail, a second TG run was performed at 4 K/min and stopped after the first mass loss. XRPD investigations of this residue proved that it is amorphous (Figure S11 in the Supporting Information). When the experiment was repeated with 1 K/min, a crystalline product was obtained, which unfortunately corresponds to the 2D compound **3/I**.

DTA-TG measurements on the hydrate complex **2** show a well-resolved TG step of 7.5% at about 78 °C, which is accompanied by an endothermic event in the DTA curve, corresponding to the removal of all water molecules (Figure 3 and Figure S10 in the Supporting Information). On further heating, the TG curves look similar to that of **1**.

When the heating is stopped after water removal and the residue is investigated by XRPD, a mixture of compound **3/I** and an additional crystalline phase is formed, which does not correspond to compound **1** or **2** (Figure S12 in the Supporting Information). In the IR spectra of this mixture the asymmetric C−N-stretching vibration is observed at 2099.5 cm^{-1}, indicating that in both crystalline phases only μ-1,3-bridging thiocyanato anions are present (Figure S13 in the Supporting Information).[16] Elemental analysis of this mixture shows that the composition is still $Co(NCS)_2(4\text{-acetylpyridine})_2$. Consequently, the additional crystalline phase (**3/II**) must be a second modification of **3/I**.

To investigate whether the new form **3/II** can be prepared phase pure, heating rate dependent measurements were performed and the residues isolated after water removal were investigated by XRPD.[17] These investigations clearly show that with decreasing the heating rate the content of **3/II** increases, but even at very low heating rates of 1 K/min the residues still contain significant amounts of **3/I** (Figure S14 in the Supporting Information).

Similar results were also found when hydrate **2** was investigated by temperature dependent XRPD measurements, where no hints were found that **3/II** can be obtained as a pure phase (Figure S15 in the Supporting Information).

DOI: 10.1021/ic503029t
Inorg. Chem. 2015, 54, 2893−2901

All the results presented above strongly indicate that the **3/II** phase is metastable and that on further heating it transforms into the more stable form **3/I**. Therefore, the hydrate **2** was annealed at temperatures much below the decomposition temperature observed in the TG measurements at 1 K/min. To our surprise, annealing for some hours at 70 °C leads to the formation of form **3/II** almost as a pure form, as no reflections of compounds **1**, **2**, and **3/I** were visible in the XRPD pattern. IR spectroscopic investigations showed that the spectra of this new form are almost identical to that of **3/I** (Figure S16 in the Supporting Information).

As stated above, the recrystallizations from different solvents always led to **3/I**, and no (single crystal) sample of **3/II** was obtained. Unfortunately, on thermal annealing only a microcrystalline powder is obtained that cannot be characterized by single crystal X-ray diffraction. However, a compound of composition $Cd(NCS)_2(4\text{-acetylpyridine})_2$ that crystallizes in two different modifications was already reported by our group, and its structures correspond to that what we expected for the Co compound.[18] Namely, in each of the two forms the Cd cations are octahedrally coordinated and are μ-1,3-bridged by pairs of thiocyanato anions into chains (Figure S17 in the Supporting Information). Obviously, for this metal cation the chain compounds are thermodynamically stable. Unfortunately, the Co compound **3/II** seems to crystallize in a different modification, because none of the Cd forms are isotypic to it. Therefore, we tried to determine the structure of **3/II** *ab initio* from XRPD data.

Crystal Structure of Compound 3/II. The XRPD pattern of **3/II** can be indexed in a triclinic unit cell with $Z = 1$ molecules in the unit cell (Table 2). The structure was solved and refined in space group $P\bar{1}$ (Figure S1 in the Supporting Information). In the crystal structure each Co cation is octahedrally coordinated by two terminal N-bonded 4-acetylpyridine coligands and four thiocyanato anions; all of them are *trans* coordinated (Figure 4).

The Co cations are linked by pairs of μ-1,3-bridging thiocyanato ligands into chains, that elongate in the direction of the crystallographic *a*-axis (Figure 4). This structure corresponds to the chain structure expected at the beginning of our investigations, which is indeed frequently observed in this family of compounds. The intrachain Co···Co distance equals 5.6280 Å, whereas the shortest interchain Co···Co distance is 8.4717 Å. The chains are arranged in a way that all $N_{acetylpyridine}$–Co–$N_{acetylpyridine}$ vectors are parallel. The phenyl rings along the chain and of neighboring chains are rotated and shifted relative to each other, which means that even in this form no significant $\pi\cdots\pi$ interactions are involved.

Investigations on the Thermodynamic Stability of 3/I and 3/II. To investigate the relative thermodynamic stability of **3/I** and **3/II**, a solvent mediated conversion experiment was performed in which a mixture of both modifications was stirred in a saturated solution in ethanol for several hours, and afterward, the residue was investigated by XRPD. All crystals of **3/II** disappeared within 3 h; afterward, only form **3/I** was present (Figure 5). This observation clearly proves that form **3/I** represents the thermodynamically stable form at room temperature, at which form **3/II** is metastable.

To investigate whether the two modifications can be transformed into each other, experiments using DSC and XRPD were performed for both forms (Figures S18–S20 in the Supporting Information). On heating **3/I**, decomposition is observed at a peak temperature T_p of 213 °C without any hint

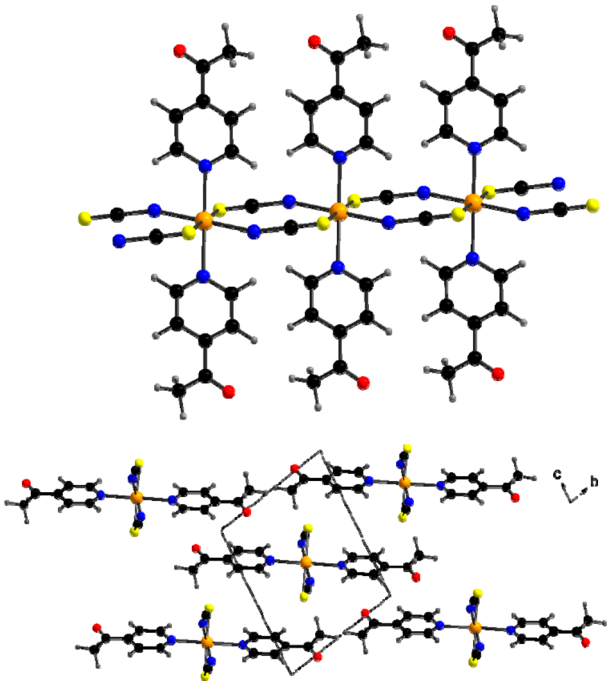

Figure 4. Crystal structure of form **3/II** with view of the Co thiocyanato chains (top) and of the arrangement of the chains with view along the crystallographic *a*-axis (bottom).

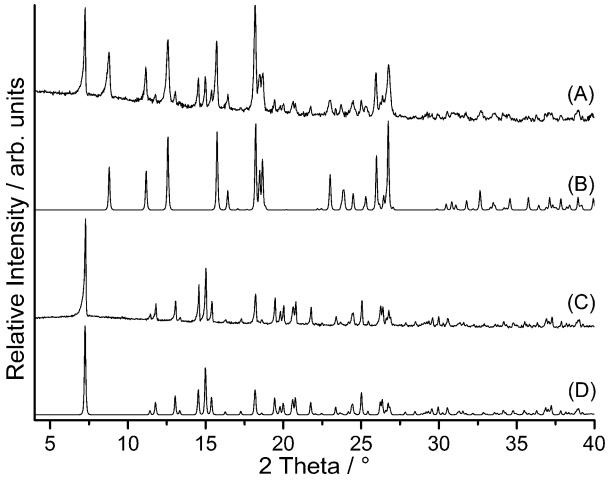

Figure 5. Experimental X-ray powder pattern of a mixture of **3/I** and **3/II** before (A), calculated powder pattern for **3/II** (B), mixture after stirring for 3 h (C), and powder pattern for **3/I** (D) calculated from single crystal data.

for a further transformation into (e.g.) **3/II** (Figure S18 in the Supporting Information). On the contrary, for **3/II** a small endothermic peak was observed at about 70 °C, but surprisingly, the XRPD pattern of a residue obtained at 80 °C corresponds to that of the pristine material **3/II**. It should be noted that the reversibility of this event was not checked.

However, on further heating an additional endothermic signal is observed at T_p = 190 °C, followed by a second strong endothermic event at 200 °C that corresponds to the decomposition of the material (Figure S19 in the Supporting Information). If the residue is isolated at 190 °C and investigated by XRPD measurements, it is proven that **3/II** has been transformed into **3/I**. This is consistent with the temperature dependent XRPD measurements shown in

DOI: 10.1021/ic503029t
Inorg. Chem. 2015, 54, 2893–2901

Supporting Information Figure S15, where the same transition is observed. Because this transition is endothermic one can assume that both forms are related by enantiotropism with **3/II** being stable at lower temperatures.

Magnetic Investigations. Compounds **1**, **2**, **3/I**, and **3/II** were investigated for their magnetic properties. For all four compounds the effective magnetic moment at 300 K reaches 4.9−5.1 μ_B per Co ion. These values are within the typical range 4.7−5.2 μ_B for the room temperature magnetic moment of the Co(II) ion in an octahedral surrounding.[19] Below 300 K the decrease of $\chi T(T)$ with decreasing temperature is an effect of Co(II) single ion properties, which is illustrated by the magnetic moment dependence for discrete complexes **1** and **2** (Figures S21 and S22 in the Supporting Information). For **1** and **2** no magnetic anomaly is observed down to 2 K. For **3/I** an additional effect is observed: the increase of $\chi T(T)$ below 20 K. This is the effect of an exchange interaction mediated through the −NCS− bridges between Co centers that create *ab* layers (Figure S23 in the Supporting Information). However, no signs of a magnetic ordering were observed. On the basis of susceptibility data measured at 100 Oe, the $\chi T(T)$ dependence changes smoothly down to 2 K. For **3/II** the exchange interaction through the anionic ligands creates a 1D system of Co(II) spins, leading to interesting magnetic properties at low temperatures. For this reason, detailed investigations of magnetic properties of this compound were undertaken and are presented below.

The magnetic susceptibility of **3/II** measured at 1 kOe leads to χT = 3.1 cm^3 K/mol at 300 K, corresponding to an effective magnetic moment of 4.98 μ_B (see Figure 6). Below 50 K the

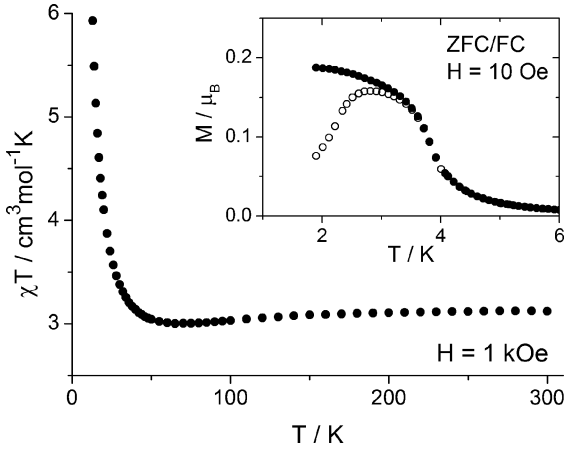

Figure 6. Temperature dependence of magnetic susceptibility of **3/II** measured at H_{DC} = 1 kOe. Figure is cut at t he top. Inset: zero-field cooled (○) and field cooled (●) magnetization at 10 Oe.

decrease expected due to single ion properties of Co(II) ions is overcome by a strong increase due to a ferromagnetic exchange interaction between Co magnetic moments. Very similar behavior was observed in a number of related Co chain compounds.[7,20] Below 10 K the susceptibility measured at the low magnetic field of 10 Oe increases significantly and saturates. The maximum slope of $\chi(T)$ is reached at 3.8 K. Zero-field cooled and field cooled magnetization curves measured at the same field bifurcate below 3.6 K (inset of Figure 6 and Figure S24 in the Supporting Information). These properties point to a kind of freezing of Co magnetic moments in **3/II** at low temperatures.

The magnetization of **3/II** measured at 1.8 K as a function of field is shown in Figure 7 with the low-field hysteresis loop

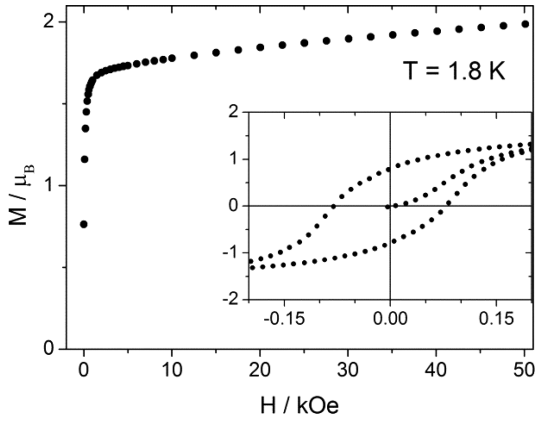

Figure 7. Field dependence of magnetization for **3/II** measured at 1.8 K. Inset: hysteresis loops measured at 1.8 K.

zoomed in the inset. The coercive field is of the order of 60 Oe, and depends slightly on the sweep rate of the magnetic field. At low fields a rapid increase is observed (up to 1.65 μ_B at 1 kOe). At higher fields the slower increase of the magnetization at higher fields (up to 2.0 μ_B at 50 kOe) is related to the strong single-ion anisotropy of Co(II).

The susceptibility data above the freezing temperature allows us to estimate the exchange interaction between Co ions. For Co^{II} in a distorted octahedral crystal field the ground 3d electron state is a Kramers doublet, and the first excited state usually has an energy higher by 100−200 cm^{-1}. In such a case, below 20 K the magnetic properties can be described assuming that each Co has the effective spin s = 1/2 with a high anisotropy. We used the model of a chain of s = 1/2 Ising spins with an exchange interaction between nearest neighbors, defined by the Hamiltonian

$$\hat{H} = -J\sum_i s_i^z s_{i+1}^z + \mu_B \sum_i \vec{H}\cdot\hat{g}\cdot\vec{s}_i \qquad (1)$$

where $\hat{g}$ tensor includes g-factors parallel and perpendicular to the deformation axis. The solution given by Fisher leads to zero-field magnetic susceptibility[21]

$$\chi_{\parallel}^{chain} = \frac{N_A g_{\parallel}^2 \mu_B^2}{4kT}\exp\left(\frac{J}{2kT}\right)$$

$$\chi_{\perp}^{chain} = \frac{N_A g_{\perp}^2 \mu_B^2}{2J}\left[\tanh\left(\frac{J}{4kT}\right) + \frac{J}{4kT}\mathrm{sech}^2\left(\frac{J}{4kT}\right)\right] \qquad (2)$$

for the field parallel and perpendicular to the easy axis of Ising spins, respectively. For $J > 0$ at low temperatures the parallel susceptibility strongly dominates and is responsible for the exponential increase of χT.

The $\ln(\chi T)$ versus $1/T$ dependence calculated using the low field susceptibility of **3/II** is shown in Figure 8. The demagnetization correction was taken into account. The linear dependence observed in the 5−20 K temperature range is in agreement with eqs 2, but below 5 K χT increases faster. This effect can be accounted for by introducing a ferromagnetic interaction between chains, quantified by the zJ' parameter in the mean field model approximation

DOI: 10.1021/ic503029t
Inorg. Chem. 2015, 54, 2893−2901

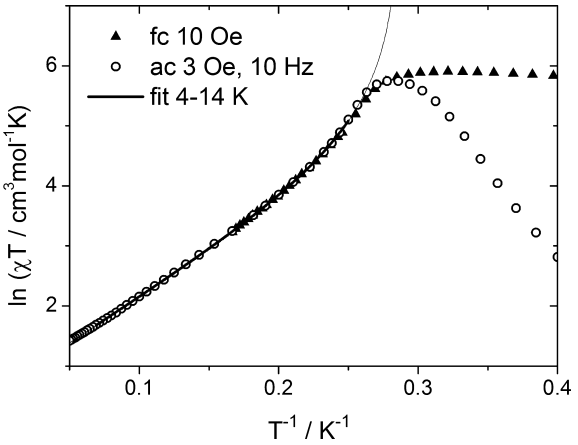

Figure 8. Low field magnetic susceptibility of **3/II**: field cooled dc data (▲) and ac data (○). The solid line is the fit and its extrapolation (see text).

$$\chi_i = \frac{\chi_i^{\text{chain}}}{1 - zJ'\chi_i^{\text{chain}}/N_A g_i^2 \mu_B^2} \quad (3)$$

For the polycrystalline sample the average susceptibility is

$$\chi = (\chi_{\parallel} + 2\chi_{\perp})/3$$

The parameters $g_{\parallel}$, J, and zJ' were fitted to reproduce the ac susceptibility data in the temperature range 4−14 K. The parameter $g_{\perp}$ was fixed to zero, which corresponds to neglecting the $\chi_{\perp}^{\text{chain}}$ term. We obtained $g_{\parallel} = 7.74(3)$, $J/k = 30.2(1)$ K, $zJ'/k = +0.18(1)$ K. The curve calculated using these parameters diverges to infinity at $T = 3.48$ K (see Figure 8). An attempt to fit the same data also including in the model $\chi_{\perp}^{\text{chain}}$ leads to $g_{\perp} = 0$, but with a huge uncertainty.

To investigate the relaxation properties of **3/II** ac susceptibility measurements were performed as a function of temperature. The ac susceptibility measured at zero dc field (shown in Figure 9) strongly depends on the driving field frequency. The peaks of in-phase susceptibility $\chi'(T)$ are accompanied by peaks of out-of-phase susceptibility χ''. All maxima significantly shift to lower temperatures with decreasing ac frequency, which is indicative for a slow relaxation of the magnetization as observed in, e.g., superparamagnets and spin glasses. The parameter φ, calculated here as the temperature shift of the χ'' peak on a decade of frequency

$$\phi = \Delta T_m/[T_m \Delta(\log f)]$$

equals 0.074, if the data at 0.1 and 1000 Hz are used to estimate the differences. This is just below the range typical for ideal superparamagnets and single chain magnets, where usually $\varphi >$ 0.1, but rather falls in the range typical for spin glasses (0.01−0.08).[22]

To get more precise information about magnetic relaxation in **3/II** we made isothermal, frequency dependent ac measurements (see Figure S25 in the Supporting Information). The Cole−Cole model was used for their analysis. The relaxation time τ was obtained for temperatures from 2.4 to 3.6 K. At lower and higher temperatures the relaxation time is beyond the available frequency window. It should be noted that the distribution of the relaxation times is broad, which is illustrated by the parameter α which varies from 0.4 to 0.52. The temperature dependence of the mean τ roughly follows the Arrhenius law $\tau = \tau_0 \exp(\Delta_\tau/kT)$, with the barrier energy Δ_τ/k = 74(3) K and $\tau_0 = 0.66$ ps (see Figure S26 in the Supporting Information). The magnetic properties of **3/II** show some features characteristic for single chain magnets (crystal structure with one-dimensional system of strongly interacting spins, weak interchain interaction, lack of obvious source of crystal disorder). Some features are characteristic for ordered ferromagnets (high magnetization at low field, nonzero interchain interaction creating a 3-dimensional magnetic network leading to a divergence of susceptibility at $T > 0$), and some features are characteristic of a cluster spin-glasses (distribution of relaxation times). To get additional insight and adjudicate if a long-range magnetic ordering transition takes place in **3/II** we measured its specific heat.

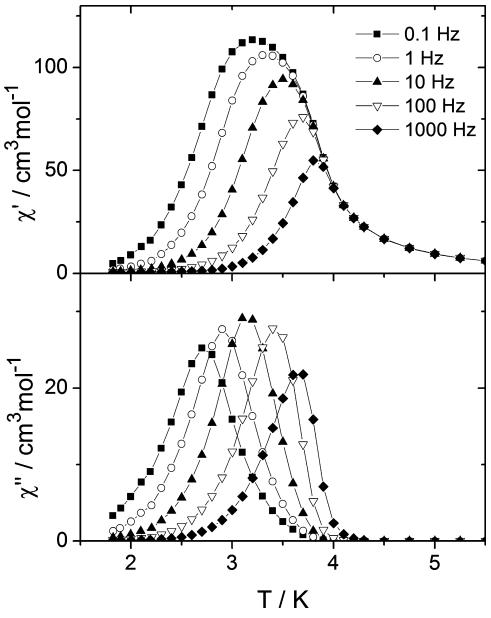

Figure 9. Temperature dependence of ac susceptibility for **3/II** measured at $H_{DC} = 0$ and $H_{AC} = 3$ Oe for different ac field frequencies from 0.1 to 1000 Hz.

Specific Heat of 3/II. The specific heat C measured in zero magnetic field is presented in Supporting Information Figure S27, while the extracted magnetic contribution C_{magn} is shown in Figure 10. A peak present at $T_c = 3.8$ K in the $C_{magn}(T)$ dependence points to an ordering transition around this temperature.

A quantitative analysis of $C(T)$ data requires estimation of the phonon contribution and the magnetic contribution to the specific heat. The phonon contribution was included using the single mode Debye model, which is the appropriate approximation in the limit of low temperatures. For this reason only data below 15 K were taken into account in further analysis. The specific heat of the chain defined by Hamiltonian (eq 1) in zero magnetic field is equal[21b]

$$C_{\text{chain}} = R(J/4kT)^2 \text{sech}^2(J/4kT)$$

where R is the gas constant. The total specific heat

$$C(T) = BC_{\text{chain}}(J, T) + AC_{\text{Debye}}(\theta_D, T)$$

used to model the experimental data of **3/II** did not include any interchain interactions, so it could not account for the ordering transition, and reproduce the peak at 3.8 K. For this reason the parameters B, J, A, and θ_D were fitted using the data in the range 4.3−15 K, i.e., above T_c. We obtained the

DOI: 10.1021/ic503029t
Inorg. Chem. 2015, 54, 2893−2901

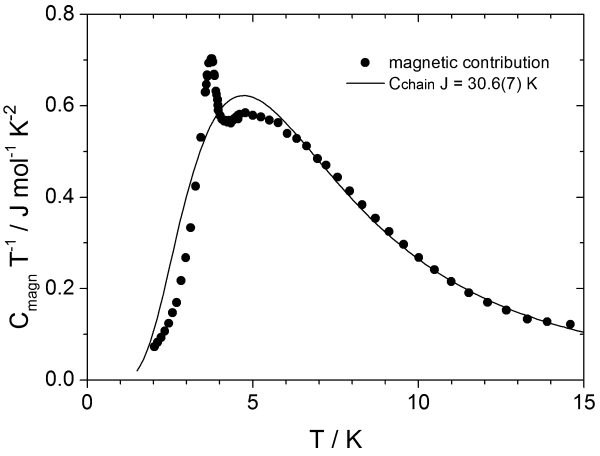

Figure 10. Magnetic contribution to the specific heat of **3/II** vs temperature. The dashed line is the fitted Ising chain contribution.

parameters J/k = 30.6(7) K, the effective Debye temperature θ_D = 82(4) K, and the factors A = 0.23(2) and B = 0.93(4). For the Ising chain, the zero field specific heat does not depend on the sign of J. The positive sign (ferromagnetic interaction) was assigned on the basis of the magnetic properties of **3/II**. The J value obtained here from specific heat data is almost identical to the value 30.2(1) K obtained from magnetic measurements.

The magnetic contribution, calculated as

$$C_{magn} = C - AC_{Debye}(\theta_D, T)$$

is shown in Figure 10. Above 4 K the fitted curve follows experimental points, confirming that magnetic properties of **3/II** can be described above this temperature using a one-dimensional model. However, at lower temperatures, the fitted $C(T)$ deviates from measured data, which denotes a crossover from 1D to 3D system, due to magnetic interactions between chains. The critical entropy, i.e., the entropy change from 0 to T_c, quantifies how ideal a 1D magnetic system is. It is zero for the 1D system, about 0.805R ln2 for 1/2 Ising spins on a simple cubic 3D lattice,[21b,23] and reaches R ln2 for a mean-field model. For **3/II** the entropy change from 2 to 3.8 K (which is close to the critical entropy, see Figure 10) is only 0.10R ln2, close to the 1D case.

The parameter B should be equal to 1.0 in the ideal case. A slightly smaller value obtained for **3/II** may have two sources. The first is a possible error of the sample mass, which we estimate to 4% on the basis of mass uncertainty. The second possible explanation is an impurity in the sample, in this case a very small fraction of **3/I**, which is indicated by the Rietveld refinement. In zero magnetic field noninteracting Co(II) ions do not add any contribution to the specific heat. If any exchange interaction between spins is present, it produces a heat capacity with a maximum at a temperature proportional to this exchange interaction. The magnetic properties of **3/I** exclude any strong exchange interactions, and predict lack of significant specific heat contribution above 2 K. This second explanation is also supported by specific heat measurements in external field (Figure S28 in the Supporting Information), where a small upturn of $C(T)$ is visible below 3 K for 10 kOe data. The external field splits the lowest Kramers doublet of isolated Co(II) giving rise to a Schottky anomaly with a maximum below 2 K. No such effect is expected for the Ising chain. However, a very small impurity of **3/I** does not influence the fitted value of J, and most importantly, the deduced fact that **3/II** orders magnetically.

CONCLUSION

In the present contribution two new compounds of the same chemical composition were prepared that show completely different coordination networks. Surprisingly, the syntheses in solution always lead to the formation of the compound with the 2D network, that was proven to represent the thermodynamically stable phase at room temperature. However, the desired 1D compound was accessible by thermal annealing of the precursor hydrate complex, and it was shown that, compared to the 2D compound, it is thermodynamically metastable. These results once again show that the synthesis of relatively simple chemical compounds can be much more difficult to achieve than expected if more polymorphic modifications are involved. To prepare the metastable phases, alternative synthetic procedures such as thermal decomposition of suitable precursor compounds must be used, as otherwise these compounds can be easily overlooked, which is highly undesirable as from a magnetic point of view the metastable compound may be much more interesting.

The metastable compound **3/II** is a quasi-one-dimensional magnetic system. The intrachain exchange interaction between Co(II) ions is mediated through $(NCS)_2$ bridges, which leads to an exchange constant J = 30.5 K, as determined both from magnetic and specific heat data. The growing correlation length in such a chain leads to strong increase of χT at low temperatures. The much weaker interchain interaction is most probably of dipolar origin, because there is neither covalent nor hydrogen bond path between the chains. In such a case the phase transition to an ordered ferromagnetic state is possible if the magnetic moments have a pronounced component perpendicular to the chain. Due to a high anisotropy of Co(II) ions in the ground state, and the fact that all local anisotropy axes of the Co ions have the same orientation in the crystal structure, the magnetic structure is most probably collinear. In spite of the clear ordering transition at T_c = 3.8 K the relaxation of magnetization is present well below the T_c. The analysis of relaxation times leads to the energy barrier 74 K, which is much higher than the values from 33 to 39 K determined for related Co−$(NCS)_2$−Co chain compounds,[9a,20] in spite of the exchange J for all these compounds being very similar. This, together with the small τ_0 prefactor and the substantial distribution of relaxation times, suggests that the objects that relax in **3/II** are not single chains, but bigger objects having a higher energy barrier in the relaxation process. The presence of magnetic domains consisting of a bundle of chains (including parts of multiple chains) may lead to the observed relaxation behavior. Such a conviction is strengthened by the fact that previously reported compounds of this family have an antiferromagnetic ground state and show a metamagnetic transition, in contrast to **3/II**, which is a ferromagnet.

ASSOCIATED CONTENT

Supporting Information

X-ray crystallographic data in CIF format. XRPD pattern, IR spectra, DTA-TG curves, and additional magnetic measurements. This material is available free of charge via the Internet at http://pubs.acs.org.

DOI: 10.1021/ic503029t
Inorg. Chem. 2015, 54, 2893−2901

AUTHOR INFORMATION

Corresponding Author

*E-mail: cnaether@ac.uni-kiel.de.

Notes

The authors declare no competing financial interest.

ACKNOWLEDGMENTS

This project was supported by the Deutsche Forschungsgemeinschaft (Project No. NA 720/5-1) and the State of Schleswig-Holstein. We thank Professor Dr. Wolfgang Bensch for access to his experimental facility. Z.T. thanks National Science Centre Poland for financial support granted under decision DEC-2013/11/B/ST3/03799. The research was in part carried out with the equipment purchased with the support of European Regional Development Fund within the Polish Innovation Economy Operational Program (POIG.02.01.00-12-023/08).

REFERENCES

(1) (a) Desiraju, G. R. *Crystal Engineering—The Design of Organic Solids*; Elsevier: Amsterdam, 1989; p 54. (b) Desiraju, G. R. *Angew. Chem., Int. Ed.* **2007**, *46*, 8342−8356. (c) Aakeröy, C. B.; Beatty, A. M. *Aust. J. Chem.* **2001**, *54*, 409−421. (d) Braga, D.; Grepioni, F.; Desiraju, G. R. *Chem. Rev.* **1998**, *98*, 1375−1406. (e) Moulton, B.; Zaworotko, M. J. *Chem. Rev.* **2001**, *101*, 1629−1658. (f) Brammer, L. *Chem. Soc. Rev.* **2004**, *33*, 476−489. (g) Zaworotko, M. J. *Chem. Soc. Rev.* **1994**, *23*, 283−288. (h) Blake, A. J.; Champness, N. R.; Hubberstey, P.; Li, W.-S.; Withersby, M. A.; Schröder, M. *Coord. Chem. Rev.* **1999**, *183*, 117−138. (i) Sharma, C. V. K. *Cryst. Growth Des.* **2002**, *2*, 465−474. (j) Zaworotko, M. J. *Nat. Chem.* **2011**, *3*, 653−653. (k) Braga, D.; Maini, L.; Polito, M.; Scaccianoce, L.; Cojazzi, G.; Grepioni, F. *Coord. Chem. Rev.* **2001**, *216*, 225−248. (l) Khlobystov, A. N.; Blake, A. J.; Champness, N. R.; Lemenovskii, D. A.; Majouga, A. G.; Zyk, N. V.; Schröder, M. *Coord. Chem. Rev.* **2001**, *222*, 155−192.

(2) (a) Braga, D.; Grepioni, F. *Chem. Soc. Rev.* **2000**, *29*, 229−238. (b) Näther, C.; Bhosekar, G.; Jeß, I. *Inorg. Chem.* **2007**, *46*, 8079−8087. (c) Näther, C.; Jeß, I. *Inorg. Chem.* **2003**, *42*, 2968−2976. (d) Wöhlert, S.; Boeckmann, J.; Jess, I.; Näther, C. *CrystEngComm* **2012**, *14*, 5412−5420. (e) Wöhlert, S.; Jess, I.; Englert, U.; Näther, C. *CrystEngComm* **2013**, *15*, 5326−5336. (f) Blake, A. J.; Brooks, N. R.; Champness, N. R.; Crew, M.; Gregory, D. H.; Hubberstey, P.; Schröder, M.; Deveson, A.; Fenske, D.; Hanton, L. R. *Chem. Commun.* **2001**, 1432−1433. (g) Barnett, S. A.; Blake, A. J.; Champness, N. R.; Wilson, C. *Chem. Commun.* **2002**, 1640−1641. (h) Batten, S. R.; Murray, K. S. *Aust. J. Chem.* **2001**, *54*, 605−609.

(3) (a) Wöhlert, S.; Boeckmann, J.; Wriedt, M.; Näther, C. *Angew. Chem., Int. Ed.* **2011**, *50*, 6920−6923. (b) Wöhlert, S.; Ruschewitz, U.; Näther, C. *Cryst. Growth Des.* **2012**, *12*, 2715−2718. (c) Wöhlert, S.; Wriedt, M.; Fic, T.; Tomkowicz, Z.; Haase, W.; Näther, C. *Inorg. Chem.* **2013**, *52*, 1061−1068. (d) Wriedt, M.; Näther, C. *Chem. Commun.* **2010**, *46*, 4707−4709.

(4) (a) Sekiya, R.; Nishikiori, S.-i. *Cryst. Growth Des.* **2011**, *11*, 5574−5591. (b) Sekiya, R.; Nishikiori, S.-i. *CrystEngComm* **2011**, *13*, 6405−6414. (c) Shi, J. M.; Chen, J. N.; Wu, C. J.; Ma, J. P. *J. Coord. Chem.* **2007**, *60*, 2009−2013.

(5) (a) Wöhlert, S.; Peters, L.; Näther, C. *Dalton Trans.* **2013**, *42*, 10746−10758. (b) Wöhlert, S.; Fink, L.; Schmidt, M.; Näther, C. *CrystEngComm* **2013**, *15*, 945−957. (c) Wöhlert, S.; Näther, C. *Eur. J. Inorg. Chem.* **2013**, *2013*, 2528−2537.

(6) (a) Boeckmann, J.; Näther, C. *Polyhedron* **2012**, *31*, 587−595. (b) Foner, S.; Frankel, R. B.; Reiff, W. M.; Wong, H.; Long, G. J. *J. Chem. Phys.* **1978**, *68*, 4781−4783.

(7) Boeckmann, J.; Näther, C. *Dalton Trans.* **2010**, *39*, 11019−11026.

(8) (a) Zhang, W.-X.; Ishikawa, R.; Breedlovea, B.; Yamashita, M. *RSC Adv.* **2013**, *3*, 3772−3798. (b) Sun, H.-L.; Wang, Z.-M.; Gao, S. *Coord. Chem. Rev.* **2010**, *254*, 1081−1100. (c) Bogani, L.; Vindigni, A.; Sessoli, R.; Gatteschi, D. *J. Mater. Chem.* **2008**, *18*, 4733−4880. (d) Caneschi, A.; Gatteschi, D.; Lalioti, N.; Sangregorio, C.; Sessoli, R.; Venturi, G.; Vindigni, A.; Rettori, A.; Pini, M. G.; Novak, M. A. *Angew. Chem., Int. Ed.* **2001**, *40*, 1760−1763. (e) Palii, A. V.; Reu, O. S.; Ostrovsky, S. M.; Klokishner, S. I.; Tsukerblat, B. S.; Sun, Z.-M.; Mao, J.-G.; Prosvirin, A. V.; Zhao, H.-H.; Dunbar, K. R. *J. Am. Chem. Soc.* **2008**, *130*, 14729−14738. (f) Feng, X.; Liu, J.; Harris, T. D.; Hill, S.; Long, J. R. *J. Am. Chem. Soc.* **2012**, *134*, 7521−7529. (g) Zhang, S.-Y.; Shi, W.; Lan, Y.; Xu, N.; Zhao, X.-Q.; Powell, A. K.; Zhao, B.; Cheng, P.; Liao, D.-Z.; Yan, S.-P. *Chem. Commun.* **2011**, *47*, 2859−2861. (h) Miyasaka, H.; Madanbashi, T.; Saitoh, A.; Motokawa, N.; Ishikawa, R.; Yamashita, M.; Bahr, S.; Wernsdorfer, W.; Clérac, R. *Chem.—Eur. J.* **2012**, *18*, 3942−3954. (i) Yang, C.-I.; Chuang, P.-H.; Lu, K.-L. *Chem. Commun.* **2011**, *47*, 4445−4447. (j) Luo, F.; Liao, Z.-w.; Song, Y.-m.; Huang, H.-x.; Tian, X.-z.; Sun, G.-m.; Zhu, Y.; Yuan, Z.-Z.; Luo, M.-b.; Liu, S.-j.; Xu, W.-y.; Feng, X.-F. *Dalton Trans.* **2011**, *40*, 12651−12655. (k) Miyasaka, H.; Takayama, K.; Saitoh, A.; Furukawa, S.; Yamashita, M.; Clérac, R. *Chem.—Eur. J.* **2010**, *16*, 3656−3662. (l) Li, Z.-X.; Zeng, Y.-F.; Ma, H.; Bu, X.-H. *Chem. Commun.* **2010**, *46*, 8540−8542. (m) Coulon, C.; Clérac, R.; Wernsdorfer, W.; Colin, T.; Miyasaka, H. *Phys. Rev. Lett.* **2009**, *102*, 164204−164207. (n) Ishikawa, R.; Katoh, K.; Breedlove, B. K.; Yamashita, M. *Inorg. Chem.* **2012**, *51*, 9123−9131. (o) Coulon, C.; Miyasaka, H.; Clérac, R. In *Single-Chain Magnets:Theoretical Approach and Experimental Systems*; Winpenny, R., Ed.; Springer: Berlin, 2006; Vol. *122*, pp 163−206. (p) Tomkowicz, Z.; Rams, M.; Bałanda, M.; Foro, S.; Nojiri, H.; Krupskaya, Y.; Kataev, V.; Büchner, B.; Nayak, S. K.; Yakhmi, J. V.; Haase, W. *Inorg. Chem.* **2012**, *51*, 9983−9994. (q) Peresypkina, E. V.; Majcher, A. M.; Rams, M.; Vostrikova, K. E. *Chem. Commun.* **2014**, *50*, 7150−7153. (r) Rams, M.; Peresypkina, E. V.; Mironov, V. S.; Wernsdorfer, W.; Vostrikova, K. E. *Inorg. Chem.* **2014**, *53*, 10291−10300.

(9) (a) Wöhlert, S.; Fic, T.; Tomkowicz, Z.; Ebbinghaus, S. G.; Rams, M.; Haase, W.; Näther, C. *Inorg. Chem.* **2013**, *52*, 12947−12957. (b) Boeckmann, J.; Näther, C. *Chem. Commun.* **2011**, *47*, 7104−7106.

(10) Boeckmann, J.; Wriedt, M.; Näther, C. *Chem.—Eur. J.* **2012**, *18*, 5284−5289.

(11) (a) Patra, G. K.; Goldberg, I. *Acta Crystallogr., Sect. E* **2001**, *57*, m483−m484. (b) Drew, M. G. B.; Gray, N. I.; Cabral, M. F.; Cabral, J. d. O. *Acta Crystallogr., Sect. C* **1985**, *41*, 1434−1437.

(12) *Topas, Vol.*; Bruker AXS: Karlsruhe, Germany, 2007.

(13) Pawley, G. *J. Appl. Crystallogr.* **1981**, *14*, 357−361.

(14) Andreev, Y. G.; MacGlashan, G. S.; Bruce, P. G. *Phys. Rev. B* **1997**, *55*, 12011−12017.

(15) Rietveld, H. *J. Appl. Crystallogr.* **1969**, *2*, 65−71.

(16) Näther, C.; Wöhlert, S.; Boeckmann, J.; Wriedt, M.; Jeß, I. *Z. Anorg. Allg. Chem.* **2013**, *639*, 2696−2714.

(17) Näther, C.; Jeß, I. *J. Solid State Chem.* **2002**, *169*, 103−112.

(18) Werner, J.; Jeß, I.; Näther, C. *Z. Naturforsch.* **2013**, *68b*, 643−652.

(19) (a) Kahn, O. *Molecular Magnetism*; VCH: Weinheim, 1993. (b) Kurmoo, M. *Chem. Soc. Rev.* **2009**, *38*, 1353−1379.

(20) Wöhlert, S.; Tomkowicz, Z.; Rams, M.; Ebbinghaus, S. G.; Fink, L.; Schmidt, M. U.; Näther, C. *Inorg. Chem.* **2014**, *53*, 8298−8310.

(21) (a) Fisher, M. E. *J. Math. Phys.* **1963**, *4*, 124−135. (b) Carlin, R. L. *Magnetochemistry*; Springer-Verlag: New York, 1986; p 166.

(22) Mydosh, J. A. *Spin Glasses: An Experimental Introduction*; Taylor and Francis: London, 1993; p 67.

(23) de Jongh, L. J.; Miedema, A. R. *Adv. Phys.* **1974**, *23*, 1.

DOI: 10.1021/ic503029t
Inorg. Chem. 2015, 54, 2893−2901